Solid State Science and Technology, Vol. 15, No 1 (2007) 30-42
ISSN 0128-7389

EFFECT OF SODIUM HYDROXIDE CONCENTRATION ON THE PHYSICOCHEMICAL CHARACTERISTIC OF α-Bi_2O_3 NANOCRYSTALS

Irmawati Ramli, Chen May Tze and Taufiq-Yap Yun Hin

Department of Chemistry, Faculty of Science,
Universiti Putra Malaysia, 43400 Serdang, Selangor Darul Ehsan

ABSTRACT

The effect of different concentration of precipitating agent on the characteristic of bismuth oxide was investigated by precipitating bismuth salt solution with sodium hydroxide. The solids obtained were oven dried at 353 K to form a mixed phases precursors. Upon calcination in air at 723 K for 5h has transformed the precursors into a highly pure α-Bi_2O_3 nanocrystals. The particles were in the nanometer range between 42 to 58 nm. The oxides were further characterized by means of XRD, SEM and FTIR. On the reduction activity study, bismuth oxide which was prepared using low concentration of NaOH has led to a better reduced activity characteristic. The oxygen removed was of chemically bonded species as reckoned by the high reduction activation energy displayed.

INTRODUCTION

Bismuth oxides are popular material for its technological applications in optical coatings, sensor technology, varistors, and polishers [1-3]. In catalysts, it is an active component for the oxidative transformation of propylene to acrolein and acrylonitrile in the presence of ammonia. This is due to its property as an oxygen provider for insertion into the allyl intermediate. The oxygen is usually terminally bonded to bismuth [4,5].
The oxide has four polymorphic forms, with two stable ones which are monoclinic α-Bi_2O_3 and cubic δ-Bi_2O_3, and two metastable phases known as tetragonal β-Bi_2O_3 and b.c.c. γ-Bi_2O_3. All these modifications possess distinct crystalline structures and physical properties [6]. Typically Bi_2O_3 is prepared via the oxidation of bismuth metal at 1073 K or thermal decomposition of carbonates or hydroxides produced by the addition of alkali metal hydroxides to bismuth salt solution [7]. However, these methods are robust and the desires to achieve to certain oxide property are always met with uncertainty. Therefore, chemical methods are the only solution for it promises the efficiency in controlling the morphology and chemical composition of prepared solids. Thus, a well designed oxide with improved property is possible. Examples of the methods are precipitation, sol-gel, hydrothermal and colloid emulsion technique. In this study, the oxides are prepared by opting precipitation method. The process involves precipitating bismuth salt solution with various concentration of sodium hydroxide as the precipitating agent. The influence of the precipitating agent concentration on the physicochemical characteristic of the material will be discussed.

Corresponding Author: irmawati@fsas.upm.edu.my

Solid State Science and Technology, Vol. 15, No 1 (2007) 30-42
ISSN 0128-7389

EXPERIMENTAL

Precipitation of Bismuth Solids

In this method, 4.85g of bismuth trinitrate pentahydrate, $Bi(NO_3)_3.5H_2O$ (Aldrich) was dissolved in 5M nitric acid (Fischer) and was later diluted with deionised water. The bismuth concentration was adjusted to be 1M. In different containers, various concentration of sodium hydroxide (Analytical UNIVAR) was prepared which was 1, 2, 3, 4 and 5M. Bismuth solution was then titrated with these precipitating agents at constant stirring and dropping rate at ambient temperature. Titration was stopped when the solution pH became constant at about pH ~13-14. The mixture was left to aged for 1 h before it was filtered and washed with deionised water. The samples were then dried in an oven at 353 K for overnight. All the dried samples were labeled as $BiO1M_{pre}$, $BiO2M_{pre}$, $BiO3M_{pre}$, $BiO4M_{pre}$, and $BiO5M_{pre}$. Immediately after drying, the samples were sent for XRD analysis to get initial information of the phase formation of the precursors. The samples were also sent for thermal analysis to get their thermal behaviour. All of the samples were later calcined in air at 723 K for 5h. All of the heat-treated particles were sent for further analysis using XRD, FTIR, SEM and TPR. The samples were labeled as BiO*x*M, where *x* is 1, 2, 3, 4 and 5 representing the different molarity of NaOH used.

Particles Characterization

Thermal analysis (DT/TGA) was carried out by employing a Mettler Toledo Model 990 instrument in a nitrogen atmosphere with a heating rate of 10 K/min. The particle crystalline structure of the precursors and calcined materials was analysed by X-ray powder diffraction (XRD) using a Shimadzu Model XRD-6000 CuK_α radiation at 40 kV and the crystallite size was evaluated using Scherrer's equation for the Bi peak. A Fourier Transform Infra Red (FTIR) spectroscopy was conducted by using Perkin Elmer 1725X spectrometer. Further inspection on the particle was done by scanning electron microscopy. The particle reduction activity and total amount of oxygen was obtained by conducting Temperature Programmed Reduction (TPR) analysis on the pretreated samples.

Corresponding Author: irmawati@fsas.upm.edu.my

Solid State Science and Technology, Vol. 15, No 1 (2007) 30-42
ISSN 0128-7389

RESULTS AND DISCUSSION

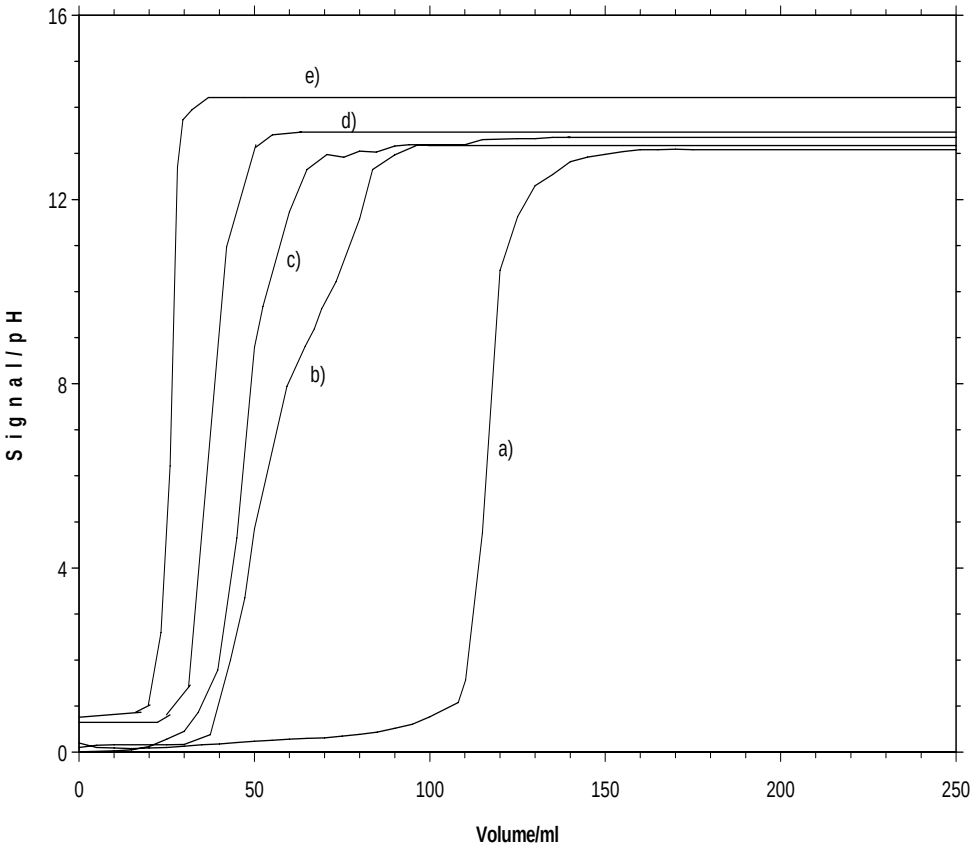

Figure. 1: Titration curves of bismuth solutions precipitated with a) 1M b) 2M c) 3M d) 4M and e) 5M sodium hydroxide.

Titration Curves

Figure. 1 shows the titration curves of all the samples. Visible precipitation is observed immediately after titration process begins in all samples. This is a clear indication that sufficient amount of hydroxyl anions are available to bind with bismuth cation. The ionic chemical equation can be represented as below.

$$Bi^{3+} + 3OH^{-} \longrightarrow Bi(OH)_3$$

The addition of more precipitating agent resulted in the formation of more cloudy solutions. As the precipitation process proceeds, pH of the solution increased continuously and the precipitate contains more and more bismuth hydroxides [8]. The pH value became constant at pH~13-14. No nucleation process is presumably occurs at this stage, instead growth process is prevail [9]. When comparing on the pH-NaOH volume response among all samples, it is clearly observed that higher concentration of precipitating agent will give faster response. This is due to the excess of OH^{-} available in the solution. In another word, nucleation process is suggested to happen very rapidly.

Corresponding Author: irmawati@fsas.upm.edu.my

Solid State Science and Technology, Vol. 15, No 1 (2007) 30-42
ISSN 0128-7389

Differential Thermal/Thermal Gravimetry Analysis (DT/TGA)

The DT/TGA thermograms of all of the precursors are shown in Figure. 2. A similar pattern is displayed by all samples in which an endothermic peak observed at 343 K is due to the evaporation of physisorbed water in the samples with percentage of weight loss is about 0.08 %. Two major weight losses are observed at temperature between 453 and 693 K. The first endotherm is due to the removal of crystalline water, ammonium and nitrate groups, whereas the second endotherm which occurs above 573 K is probably due to the decomposition of remaining ammonium and nitrate groups [10]. Thus, a calcination temperature of 723K was found sufficient to transform the mixed phases into bismuth trioxide phase [11].

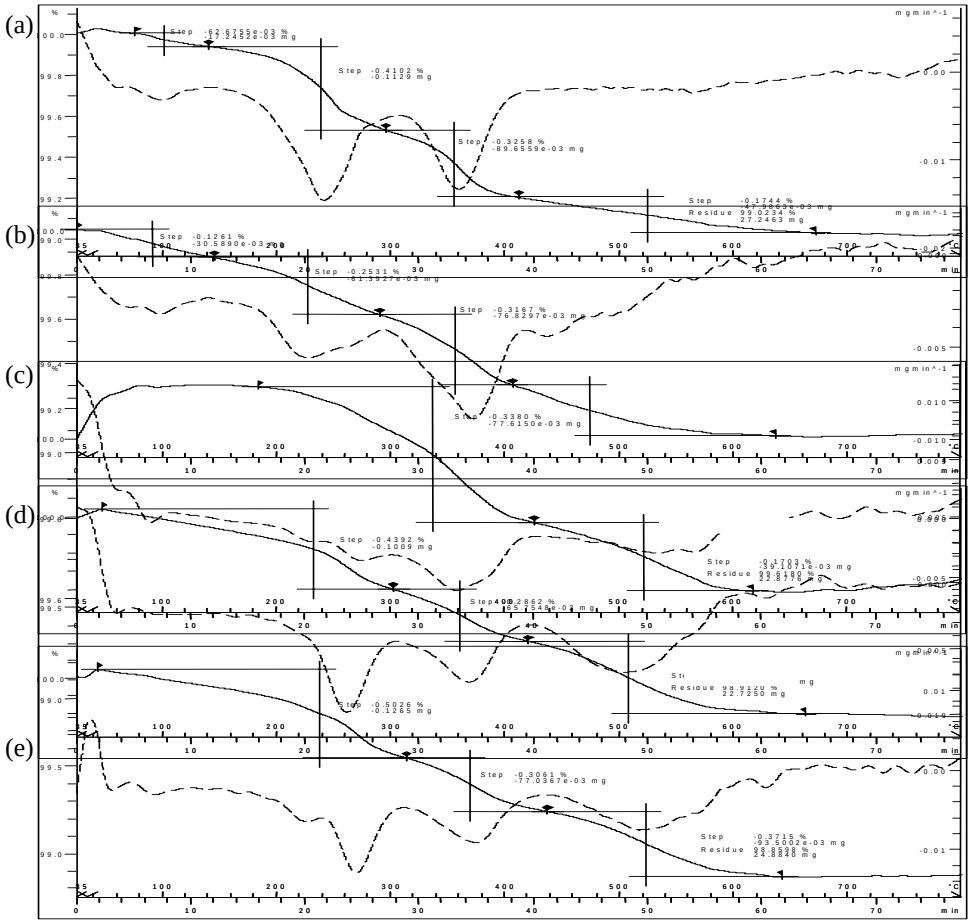

Figure. 2: DT/TGA thermograms for precursors a) $BiO1M_{pre}$ b) $BiO2M_{pre}$ c) $BiO3M_{pre}$ d) $BiO4M_{pre}$ e) $BiO5M_{pre}$.

Corresponding Author: irmawati@fsas.upm.edu.my

Solid State Science and Technology, Vol. 15, No 1 (2007) 30-42
ISSN 0128-7389

X-Ray Diffraction (XRD)

The XRD diffractograms of precursors and calcined samples are shown in Figure. 3 and Figure. 4, respectively. For the former, the peaks are sharp and intense, an indication that the precursors are highly crystalline. Main peaks are observed at 2θ = 25.7°, 26.9°, 27.4°, 28.0°, 33.2°, and 46.3° which are referred to α-Bi_20_3 phase. Bismuth oxide nitrate hydroxide hydrate phase, $Bi_6O_4(NO_3)_5(OH)_5.0.5H_20$ (JCPDS File no. 6-0504) is present at 2θ = 35.3°, 37.5° and 52.9° and sodium bismuth oxide, Na_3BiO_4 is observed at 2θ = 29.3°, 30.1°, 34.9°, 54.4° and 58.4°. This data clearly showed that the precursors exist as mixed phases. Still, the evolution of α-Bi_2O_3 phase is the most prominent.

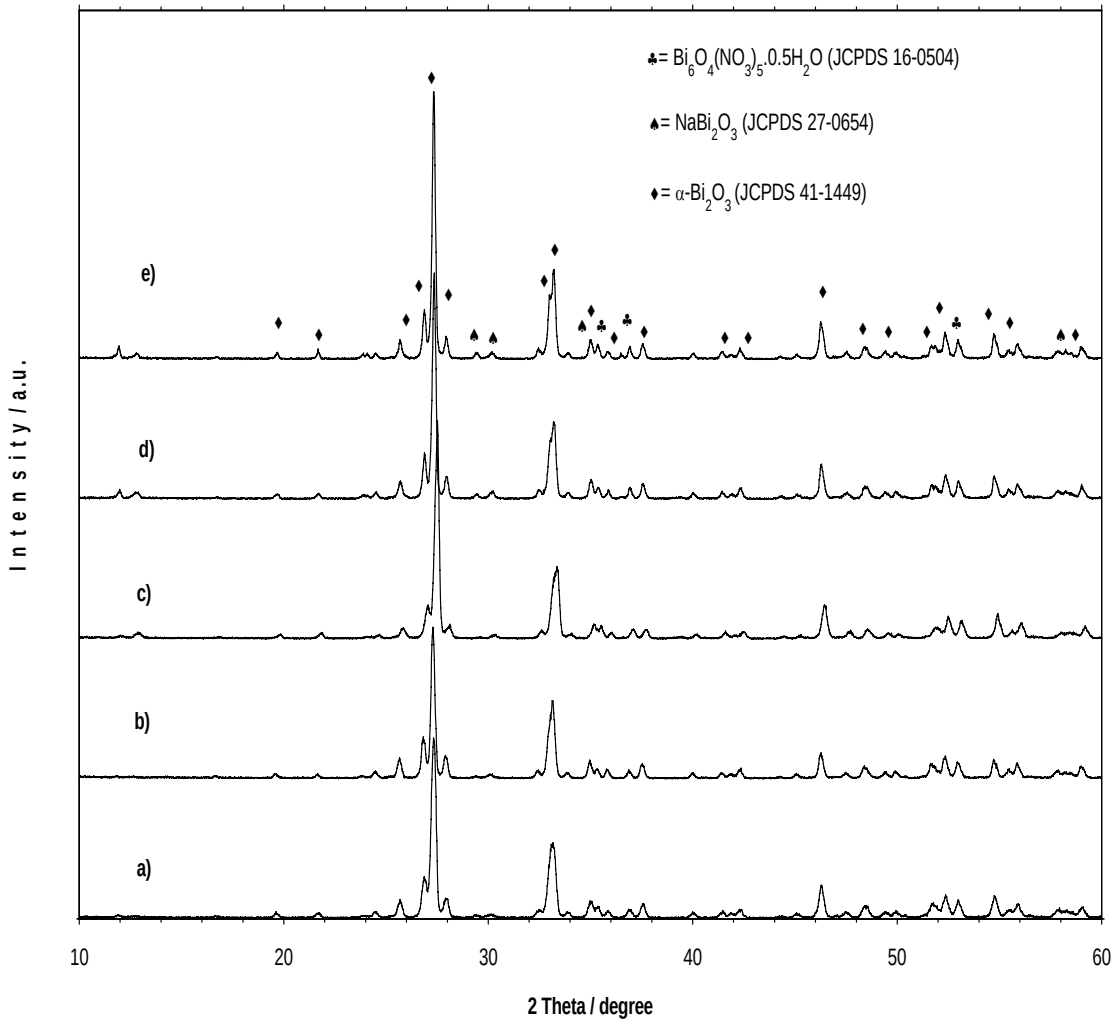

Figure. 3: XRD patterns of precursors a) BiO1Mpre b) BiO2Mpre c) BiO3Mpre d) BiO4Mpre e) BiO5Mpre.

Corresponding Author: irmawati@fsas.upm.edu.my

Solid State Science and Technology, Vol. 15, No 1 (2007) 30-42
ISSN 0128-7389

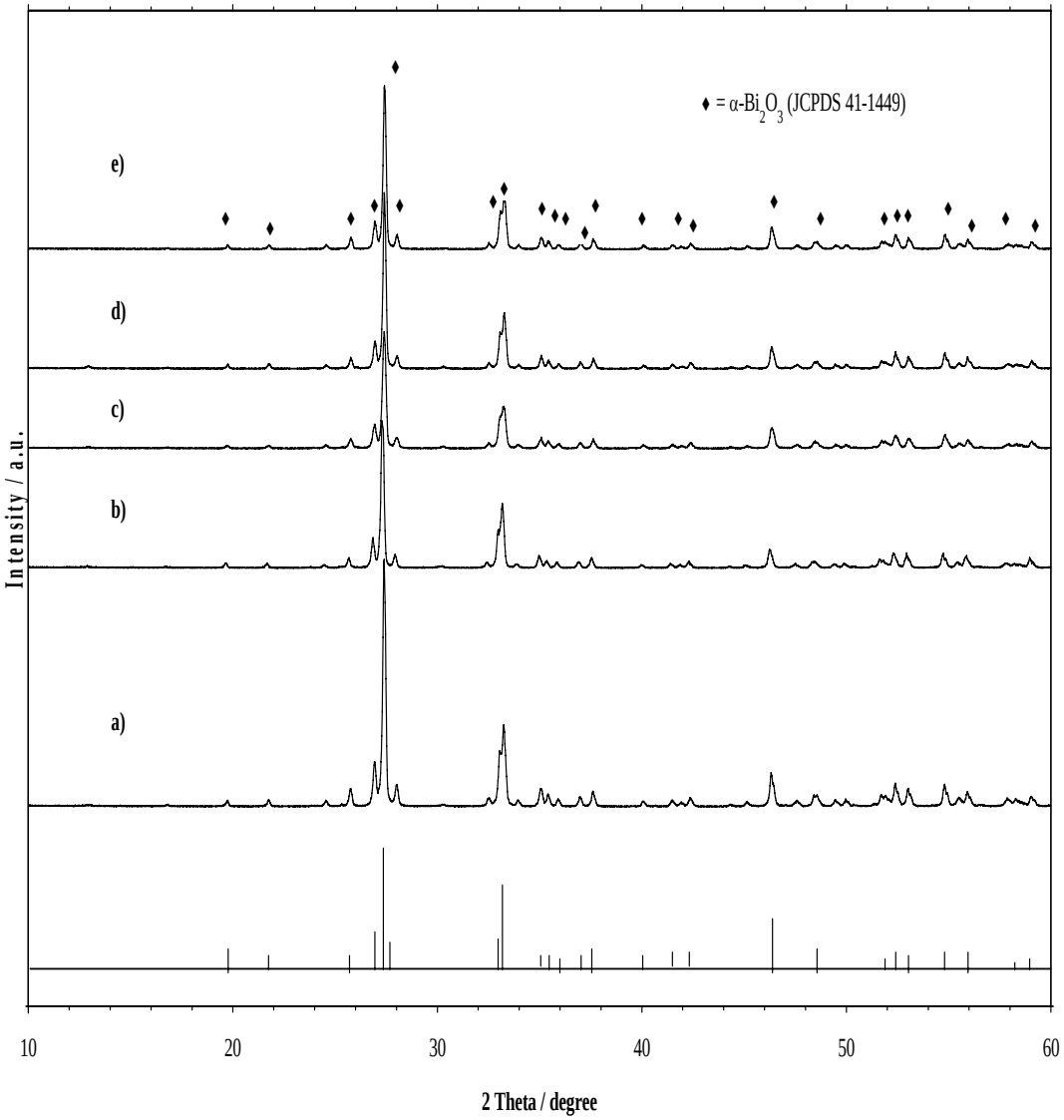

Figure. 4: XRD patterns of calcined samples a) BiO1M b) BiO2M c) BiO3M d) BiO4M e) BiO5M.

Once the precursors were heat-treated in air for 5 h at 723K, a pure α-Bi_2O_3 phase is produced. This can be evidenced in Figure. 4 which shows diffractograms which are match perfectly with the reference data of α-Bi_2O_3 (JCPDS File no. 41-1449). Thereby, calcination process has shown to be an efficient treatment process to convert impure sample into its pure form by eliminating all of the unwanted species. The three most prominent peak at 2θ = 27.4°, 33.3° and 46.3° correspond to (120), (200) and (041) reflection. The crystal plane is bismite and the crystal system is monoclinic. Estimation of the crystallite size based on X-ray peaks broadening was calculated using Debye-Scherrer equation as shown below [12, 13].

Corresponding Author: irmawati@fsas.upm.edu.my

$$t = \frac{0.9\chi}{\beta_{hkl} \cos \theta_{hkl}}$$

where t is the crystallite size for *(hkl)* phase, χ is the X-ray wavelength of radiation for CuK_α, β_{hkl} is the full-width at half-maximum (FWHM) at (*hkl*) peak in radian and θ_{hkl} is the diffraction angle for (*hkl*) phase.
The crystallite size of the (120), (200) and (041) planes of all the samples is presented in Table 1. There is no clear pattern that can be gathered on the effect of various concentration of precipitating agent on bismuth oxide crystallite size. The calculated particle size is in the nanometer range of 42 to 58 nm.

Table 1: Calculated crystallite size based on X-ray peaks broadening.

Samples	$FWHM_{120}$ [a]	t_{120} [d] (nm)	$FWHM_{200}$ [b]	t_{200} [d] (nm)	$FWHM_{041}$ [c]	t_{041} [d] (nm)
BiO1M	0.1469	55.66	0.1434	57.81	0.1532	56.40
BiO2M	0.1480	55.25	0.1842	45.00	0.1811	47.73
BiO3M	0.1921	42.56	0.1952	42.47	0.2054	42.07
BiO4M	0.1447	56.51	0.1918	43.22	0.1644	52.54
BiO5M	0.1506	54.29	0.1662	49.89	0.1619	53.37

[a] FWHM for (120) phases of Bi_2O_3
[b] FWHM for (200) phases of Bi_2O_3
[c] FWHM for (041) phases of Bi_2O_3
[d] Crystallite size by means of Debye-Scherrer's formula

Fourier Transform Infrared (FTIR) Spectroscopy
Results obtained from FTIR are useful to corroborate the evidence gathered in XRD. The FTIR spectra of the calcined particle are shown in Figure. 5. The spectra display a strong absorption band in the 600-400 cm^{-1} range, due to the Bi-O stretching mode. Also, Bi-O bending mode can be found in the same range. This was suggested by Carrazan et al. [14] in which they indicated that in the 600-400 cm^{-1} range, the stretching and deformation modes of Bi-O are expected.

Corresponding Author: irmawati@fsas.upm.edu.my

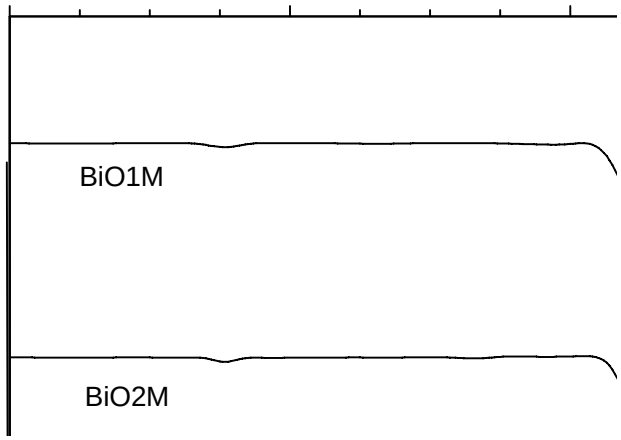

Figure. 5: FT-IR spectrum of BiO1M, BiO2M, BiO3M, BiO4M and BiO5M samples

Corresponding Author: irmawati@fsas.upm.edu.my

Table 2: FTIR lattice vibration of the samples prepared.

Samples	Range, cm^{-1}	Wavelength, cm^{-1}	Assignment
BiO1M	600-400	426 473 534	Bi - O
BiO2M	600-400	428 472 526	Bi - O
BiO3M	600-400	428 526	Bi - O
BiO4M	600-400	426 472 530	Bi - O
BiO5M	600-400	426 472 528	Bi - O

Scanning Electron Microscopy (SEM)

The SEM images of the samples are shown in Figure. 6. It is clearly seen that the particles are needles which are generally in uniform size and shape. They show sharp edges and angular corner confirming that the particles are in highly crystalline form. This is in agreement with XRD analysis which indicates that the diffraction pattern observed was referred to monoclinic system. In a work by Yang et al. [15], they also obtained a non-agglomerated Bi_2O_3 needles when prepared using $Bi(NO_3)_3.5H_2O$ and $Bi(OH)_3$ as starting material. In their work they used hydrothermal method. They claim that the formation of Bi_2O_3 needles is mainly affected by the hydroxyl anion. This result is also in line with our other work [11]. In that study, we observed that the oxides, which were prepared by precipitation method, displayed needles morphology. The precipitating agent used was NaOH which provides the hydroxyl ions readily in the solution.

Corresponding Author: irmawati@fsas.upm.edu.my

Solid State Science and Technology, Vol. 15, No 1 (2007) 30-42
ISSN 0128-7389

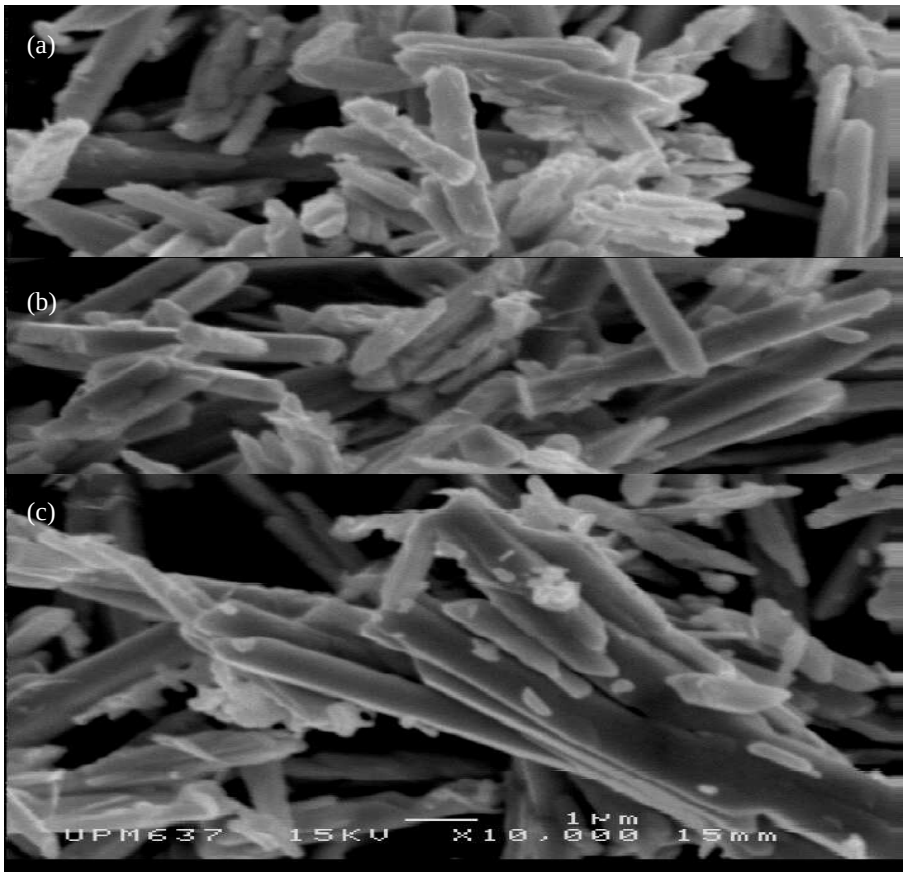

Figure. 6: SEM image of samples a) BiO1M b) BiO3M c) BiO5M (x10,000)

Temperature Programmed Reduction (TPR)

The temperature at which oxygen species are removed from the surface of a heated solid obviously reflects the strength of the surface oxygen bond. As the temperature goes higher then surface-oxygen bond is stronger. Apart from that, the analysis can give information on the total amount of oxygen species that is removable from the sample.

TPR was conducted by flowing H_2/Ar (5 % hydrogen) stream over the sample and the temperature was raised from room temperature to 1073 K at a heating rate of 5 K/min. Hydrogen from the gas phase will adsorbed on the sample surface and interact with the oxygen species which after reaching certain limit desorbed as water molecule. The reaction equation can be presented as below.

$$H_{2\,(a)} + O_{(s)} \longrightarrow H_2O_{(g)} + \square$$

Where $_{(a)}$, $_{(s)}$ and $_{(g)}$ denotes adsorb, surface and gaseous species and $\square$ is an oxygen vacancy.

The TPR profiles of the samples are shown in Figure. 7. While the temperature of peak maximum together with the reduction activation energy, E_r value and the amount of oxygen atom removed are listed in Table 3.

Corresponding Author: irmawati@fsas.upm.edu.my

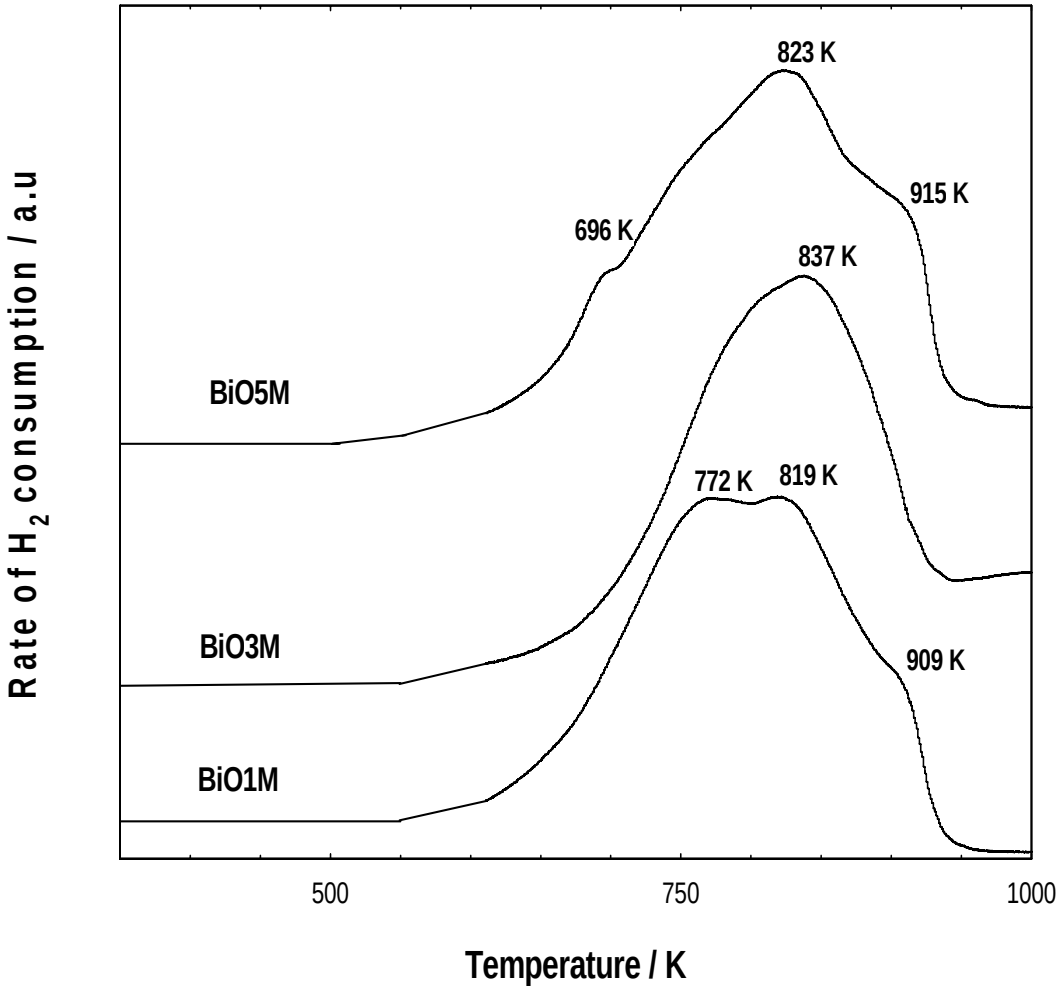

Fi

Figure. 7: TPR profile of BiO1M, BiO3M and BiO5M.

Corresponding Author: irmawati@fsas.upm.edu.my

Table 3: Total amount of oxygen atoms removed from the samples and the value of reduction activation energy, E_r.

Peaks	T_m (K)	Reduction Activation Energy, E_r ($kJmol^{-1}$)	Oxygen atom removed from the catalyst ($mol\ g^{-1}$)	Oxygen atom removed from the catalyst ($atom\ g^{-1}$)
BiO1M				
1	772	129	2.8×10^{-3}	1.7×10^{21}
2	819	137	2.1×10^{-3}	1.2×10^{21}
3	909	152	4.3×10^{-4}	2.6×10^{20}
		Total oxygen atoms removed	$\mathbf{2.3 \times 10^{-3}}$	$\mathbf{3.2 \times 10^{21}}$
BiO3M				
1	837	140	4.9×10^{-3}	2.9×10^{21}
		Total oxygen atoms removed	$\mathbf{4.9 \times 10^{-3}}$	$\mathbf{2.9 \times 10^{21}}$
BiO5M				
1	696	135	6.6×10^{-4}	3.9×10^{21}
2	823	138	2.8×10^{-3}	1.7×10^{21}
3	915	153	8.8×10^{-4}	5.3×10^{21}
		Total oxygen atoms removed	$\mathbf{4.4 \times 10^{-3}}$	$\mathbf{2.6 \times 10^{21}}$

One peak could be distinguished on the TPR curves, as shown in Figure. 7 which occur at temperature ~ 825 K. Therefore, the oxygen species evolved from all of the samples at this peak maxima could be the same one. Total amount of oxygen removed from the samples were 3.2×10^{21} $atomg^{-1}$, 2.9×10^{21} $atomg^{-1}$ and 2.6×10^{21} $atomg^{-1}$ for sample BiO1M, BiO3M and BiO5m, respectively. A slightly higher amount of oxygen atoms were successfully removed from BiO1M, followed by BiO3M and BiO5M indicating of the increase of reduced activity for the sample which was prepared when using low concentration of sodium hydroxide, thus better dispersion of bismuth oxide particles. The reduction activation energy for all samples were found to be more than 130 kJ/mol. This is a high activation energy which indicates that the oxygen species were strongly bonded to the surface of the oxide. No physisorbed oxygen species can be gathered at this high temperature regime, instead chemisorbed oxygen was found.

CONCLUSIONS

Variation in precipitating agent has shown to have an effect on the physicochemical properties of bismuth oxide particles. Fast pH-volume response was observed when higher concentration of sodium hydroxide was used, which leads to shorter time of particle production. On the other hand, low concentration of precipitating agent allows a rather delayed nucleation process, thus promise a better dispersion of particles. The oxides were found to form through bismuth oxide nitrate hydroxide hydrate route,

Corresponding Author: irmawati@fsas.upm.edu.my

which upon calcinations at 723 K in air transformed the solids into a highly pure bismuth oxide crystals with its size is the range between 42 to 58 nm. The particles were monoclinic with needle morphology. A clear effect of precipitating agent concentration on bismuth oxide can be sought from TPR analysis which shows a better reduced activity for sample which was prepared at low concentration of precipitating agent.

REFERENCES

[1]. Bandoli G., Barecca D., Brescacin E., Rizzi G.A., Tondello E., *Chem. Vap. Depos.* **2** (9) (1996) 238.
[2]. Hyodo T., Kanazawa E., Takao Y., Shimizu Y., Egashira M., *Electrochemistry* **68** (1) (2000) 24.
[3]. Adamian Z.N., Abovian H.V., Araoutiounian V.M., *Sens. Actuators B*, **35**/**36** (1996) 241-243
[4]. Arora N., Deo G., Wachs I.E., Hirt A.M., *J. Catal*., **159** (1996) 1-13
[5]. Hanna T.A., *Coord. Chem. Rev*., **248** (5-6) (2004) 429-440.
[6]. Leontie L., Caraman M., Delibas M., Rusu G.I., *Mater. Res. Bull*., **36** (2001) 1629-1637.
[7]. Keuger J., Winkler P., Luderitz E., Luck M., Wolf H.U., 'Bismuth, bismuth alloys, and bismuth compounds, in: Ullmann's Encyslopedia of Industrial Chemistry', Wiley-VCH Verlag GmbH, Weinheim, Germany, (2000).
[8]. Szabo Z.G., Kallo D., 'Contact Catalysis', vol. 2, Elsevier, Hungary (1976) pp. 45-47.
[9]. Schüth F., Unger K., 'Precipitation and Co-precipitation, Handbook of Heterogeneous Catalysis', Wiley-VCH, Germany (1997) pp. 78.
[10]. Lee M.T., Croenenbroeck J.V., Driessche I.V., Hoste S., *Appl. Catal. A: General* **249** (2003) 355-364.
[11]. R. Irmawati, M.N. Noorfarizan Nasriah, Y.H. Taufiq-Yap, S.B. Abdul Hamid, *Catal. Today*, **93-95** (2004) 701-709.
[12]. Klug P.H., Alexander L.E., 'X-ray Diffraction Procedures for Polycrystalline and Amorphous Materials', Wiley, New York (1974) pp 618.
[13]. Prasad N.S., Varma K.B.R., *Mater. Sci. Eng. B* **90** (2000) 246-253.
[14]. S.R.G. Carrazan, C. Martin, V. Rives, R. Vidal, *Spectrochim. Acta Part A* **52** (1996) 1107-1118.
[15]. Yang Q., Li Y., Yin Q., Wang P., Cheng Y., *Mater. Lett*. **55** (2002) 46-49.

Corresponding Author: irmawati@fsas.upm.edu.my